Macromolecules

Article

pubs.acs.org/Macromolecules

Interfacial Interactions between Poly(3-hexylthiophene) and Substrates

Yan Guo, Xiaojing Ma, and Zhaohui Su*

State Key Laboratory of Polymer Physics and Chemistry, Changchun Institute of Applied Chemistry, Chinese Academy of Sciences, 5625 Renmin Street, Changchun 130022, People's Republic of China

Supporting Information

ABSTRACT: Interfacial interactions between poly(3-hexylthiophene) (P3HT) and substrate surface have been investigated. P3HT nanowhiskers of single molecule thickness were prepared from chloroform solution, and their adsorption on substrates of various surface chemistries was investigated using atomic force microscopy (AFM) and Raman spectroscopy. P3HT monolayer nanowhiskers with edge-on molecular orientation were found to adsorb readily onto a SiO_2 substrate, and the amount of adsorption was significantly higher on a SiO_2 surface modified with a perfluorohexyl monolayer; no P3HT adsorption was observed on a hexyl monolayer. These results suggest that electron-withdrawing groups rather than surface energy govern the interfacial interactions. On a highly oriented pyrolytic graphite (HOPG) surface, P3HT molecules adsorbed in face-on orientation, and edge-on monolayer nanowhiskers were absent on the surface. Raman spectroscopy data revealed strong charge-transfer interactions between face-on P3HT molecules and the HOPG surface.

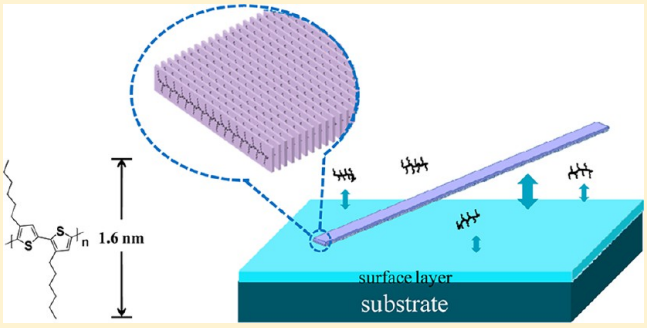

INTRODUCTION

π-Conjugated materials have been the subject of intense recent research due to their potential application in cost-efficient, solution-processable, and flexible electronic and optoelectronic devices, such as field effect transistors (FETs) and solar cells.[1,2] One of these materials is regioregular poly(3-hexylthiophene) (P3HT). It is a conjugated polymer with one of the highest charge transport mobilities reported for organic FETs (OFETs),[3,4] and its blends with carbon materials, mostly fullerene derivatives, are among the systems exhibiting highest power conversion efficiencies for polymer solar cells.[5] The performance of these devices depends not only on the molecular structure of the semiconductor but also on the film morphology.[6−8] Therefore, persistent attention has been paid to the morphology of the organic semiconductor film formed during processing, and various methods, including interface engineering, precrystallization, and post-treatment, have been employed to control the film morphology and optimize the device performance.[9−11]

It has become clear that charge transport in OFETs depends on the morphology in the first few molecular layers at the interface between the semiconductor and the insulator.[12,13] Consequently, one of the most effective ways to fabricate OFETs of high performance is to functionalize the dielectric (e.g., silicon dioxide) surface with self-assembled monolayers (SAMs).[3,9,14] OFET properties thus optimized include charge carrier mobility and threshold voltage.[15−18] In particular, dielectric surfaces functionalized with perfluoroalkyl groups were found to enhance field effect mobility in FET devices.[15,18] When processed into thin films, sheetlike P3HT molecules often self-organize into a lamellar structure where, depending on processing conditions, P3HT molecules can adopt either parallel (face-on) and perpendicular (edge-on) orientations with respect to the substrate. Sirringhaus and co-workers discovered that the field-effect mobility of films with edge-on orientation is 2 orders of magnitude larger than that with face-on orientation,[19] and since then, control of P3HT orientation in thin films on substrates has been investigated by many researchers. For example, in a series of papers, Cho and co-workers reported that P3HT adopts an edge-on and face-on orientation, respectively, on substrates with amino and alkyl functionalities and attributed these structures to different interactions between P3HT and the two surfaces.[20−22] More recently, Anglin and co-workers investigated P3HT coated on various SAMs and argued that low surface energy dielectrics, such as perfluoroalkyl monolayers, lead to edge-on orientation of P3HT molecules and consequently higher field-effect mobilities.[23] Malliaras and co-workers also reported enhanced charge carrier mobilities on perfluoroalkyl-functionalized Al_2O_3 dielectric and attributed it to interactions between the fluoroalkyl groups and the P3HT molecules at the interface.[24] While it is established that SAMs can lead to higher carrier mobilities, the molecular explanation for this phenomenon is far from clear. This largely stems from the fact that morphology

Received: December 26, 2012
Revised: March 13, 2013
Published: March 27, 2013

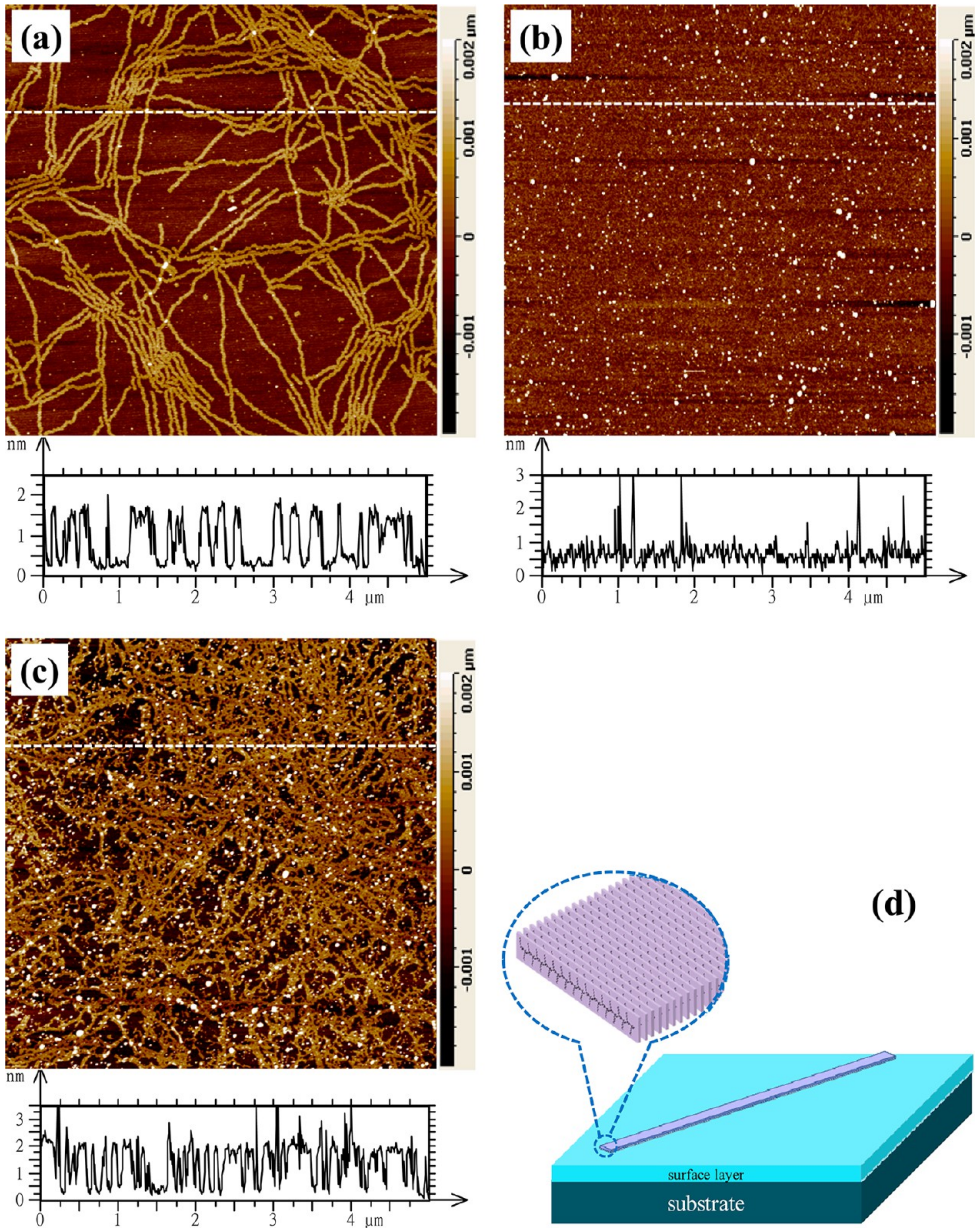

Figure 1. AFM topography images ($5 \times 5\ \mu m^2$) of P3HT nanowhiskers on (a) SiO_2, (b) C_6H_{13}, and (c) C_6F_{13} surfaces. The scale bars are shown at the right; the corresponding cross section is depicted below each image. (d) A schematic illustration of a nanowhisker adsorbed on the surface.

of spin-coated P3HT films is very sensitive to processing conditions, and there is no easy way to separate the overlying material and assess the narrow semiconductor−dielectric interfacial region directly.

Recently, we discovered that P3HT nanowhiskers of single molecule thickness can be grown from slightly oversaturated solution under mild conditions.[25] These nanowhiskers are tens of micrometers long, ~30 nm wide, and only 1.6 nm high and can be deposited on substrates in edge-on molecular orientation due to large aspect ratios of the assembly structure. Deposition of such monolayer nanowhiskers on a substrate provides an exposed interfacial layer of P3HT exclusively in edge-on orientation, which is not obscured by overlying material and thus can be readily assessed. In the present paper, we investigate the adsorption of P3HT to Si wafers with different surface functionalities in order to better understand the interactions between the surface and the P3HT interfacial layer.

EXPERIMENTAL SECTION

Materials. Regioregular poly(3-hexylthiophene) (P3HT) was purchased from Rieke Metals Inc. and used without further purification. Molecular weight (M_w = 32 000, PDI = 1.9) values were obtained by gel permeation chromatography with THF as solvent against monodisperse polystyrene standards. H−T regioregularity was determined using nuclear magnetic resonance to be about 98% by comparing the signals at 2.8 and 2.6 ppm.[19] P3HT was dissolved in refluxing $CHCl_3$ with stirring (0.1 mg mL^{-1}), and the solution was stored in darkness at 20 ± 2 °C for 1 week; a freshly prepared solution was used as comparison. Hexyltrimethoxysilane and tricholoro(1*H*,1*H*,2*H*,2*H*-perfluorooctyl)silane were purchased from Tokyo Chemical Industry Co. and Sigma-Aldrich Co., respectively, and used without further purification. Water was purified with a PGeneral GWA-UN4 unit (18.2 MΩ·cm).

dx.doi.org/10.1021/ma302645m | *Macromolecules* 2013, 46, 2733−2739

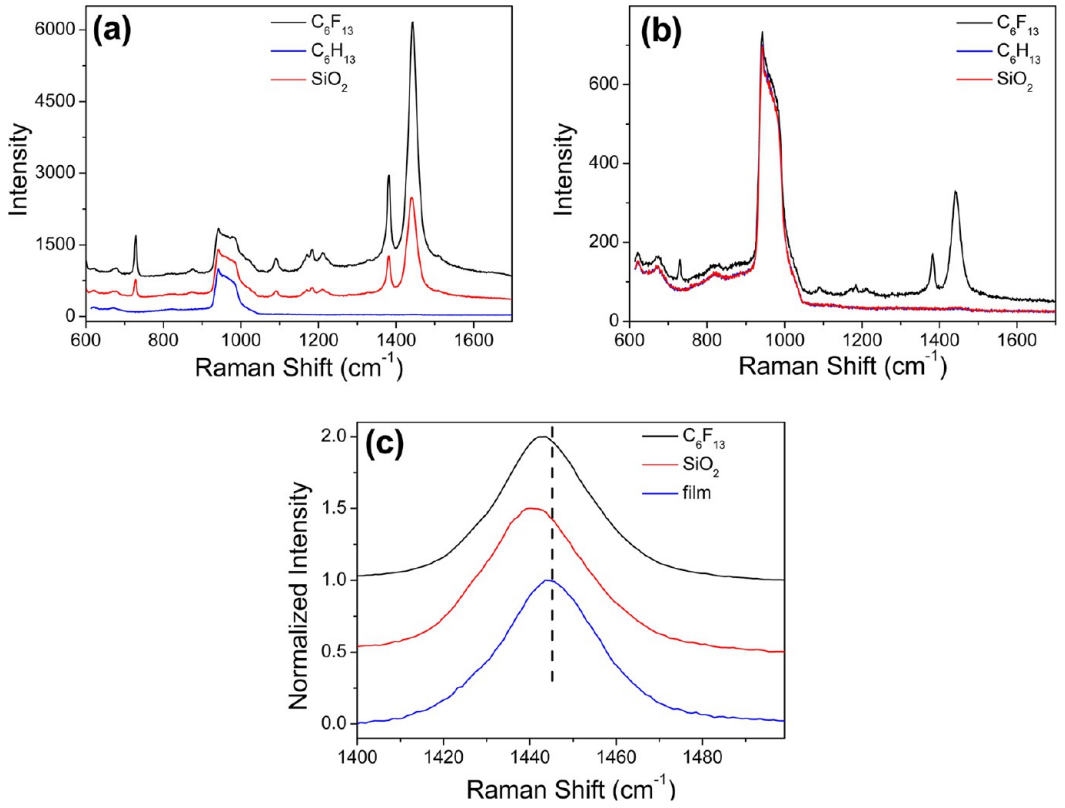

Figure 2. Raman spectra of P3HT adsorbed on different substrates from (a) an aged solution containing nanowhiskers and (b) a freshly prepared solution. The broad band at 900−1040 cm^{-1} is attributed to Si. (c) The C═C stretching band of P3HT on C_6F_{13}, SiO_2 surfaces, and a spin-coated P3HT film in the 1400−1500 cm^{-1} region; the intensities are normalized for comparison, and the dashed line marks the peak position of 1445 cm^{-1}.

Substrate Preparation and Adsorption. Silicon wafers were cleaned in a boiling piranha solution (H_2SO_4/H_2O_2 = 70:30 v/v) and rinsed with adequate ultrapure water. Cleaned silicon wafers were functionalized with hexyl and fluoroalkyl monolayer by chemical vapor deposition of hexyltrimethoxysilane and tricholoro(1*H*,1*H*,2*H*,2*H*-perfluorooctyl)silane, respectively, following a literature procedure.[15] In brief, silicon wafers were placed in a glass reactor in an oven, and 0.1 mL of the silane was injected into the reactor without direct contact with the wafer. The oven was maintained at 120 °C for 3 h to allow the silane vapor to react with the wafer surface. Then the treated wafers were heated to 140 °C for 2 h to remove unreacted silane. Highly oriented pyrolytic graphite (HOPG) surface were freshly cleaved using adhesive tape. All substrates were vertically dipped into a P3HT solution for 1 min and then immediately immersed in chloroform for 1 min.

Characterization. AFM images were obtained on an Agilent 5500 scanning probe microscope in tapping mode with Si tips with a radius of <10 nm and a resonance frequency of 250−300 kHz. Raman spectra were recorded in backscattering geometry using LabRam HR 800 (HORIBA Jobin Yvon) coupled with an Olympus BX 41 microscope; the confocal hole and the silt width were both fixed at 200 μm. Three excitation wavelengthes were used: 785 nm (YAG laser, 3.4 mW), 633 nm (He−Ne laser, 1.8 mW), and 532 nm (laser diode, 14.7 mW); all lasers were focused on the sample with a 100× objective lens (0.90 NA). Raman signals were dispersed with a 600 lines/mm grating and collected by a charge-coupled device (CCD) camera. The spectrometer was calibrated with the 520.7 cm^{-1} band of a Si standard. Each spectrum was an average of three acquisitions, each with an exposure time of 10 s. Contact angles were measured with a Ramé-Hart 200-F1 goniometer.

RESULTS AND DISCUSSION

Three Si surfaces were investigated in this study: pristine Si wafer, with a bare SiO_2 surface layer (SiO_2), and Si wafers functionalized with hexyltrimethoxysilane and tricholoro-(1*H*,1*H*,2*H*,2*H*-perfluorooctyl)silane, referred to as C_6H_{13} and C_6F_{13}, respectively. The static water contact angles were ∼0°, 95°, and 110° for SiO_2, C_6H_{13}, and C_6F_{13} surfaces, respectively, indicating a decreasing trend in surface energy. As we recently demonstrated, in a slightly oversaturated P3HT solution, thermodynamically more stable extended-chain crystals can grow slowly under mild conditions; the hexyl side chains are more soluble and the van der Waals interactions between them much weaker compared to the thienyl main chains, so that crystal growth along the side chain direction is prohibited, resulting in crystals of monolayer thickness dispersed in the solution.[25] Also in the solution are dissolved P3HT molecules. Si wafers were submerged in such a solution for 1 min, removed, and immediately rinsed with chloroform for 1 min before drying. The solvent rinsing removes residual solution from the substrate surface and ensures that any P3HT present on the surface is due to adsorption from the solution rather than precipitation from drying residual solution. Figure 1 shows the AFM topography images. On the SiO_2 substrate, a network of nanowhiskers of ∼1.6 nm thick is clearly observed, with no amorphous material present, confirming the adsorption of edge-on P3HT monolayer to the surface (Figure 1a). In contrast, on the C_6H_{13} surface, a surface with lower surface energy, no P3HT nanowhisker is present (Figure 1b). But in Figure 1c, much more P3HT nanowhiskers are seen to adsorb to the C_6F_{13}, a surface with the lowest surface energy of the three. The corresponding cross-section profile shows that the thickness of the nanowhiskers is ∼1.8 nm, slightly larger than that on SiO_2 surface, probably due to the presence of the SAM. A schematic of the arrangement of a nanowhisker adsorbed on

dx.doi.org/10.1021/ma302645m | *Macromolecules* 2013, 46, 2733−2739

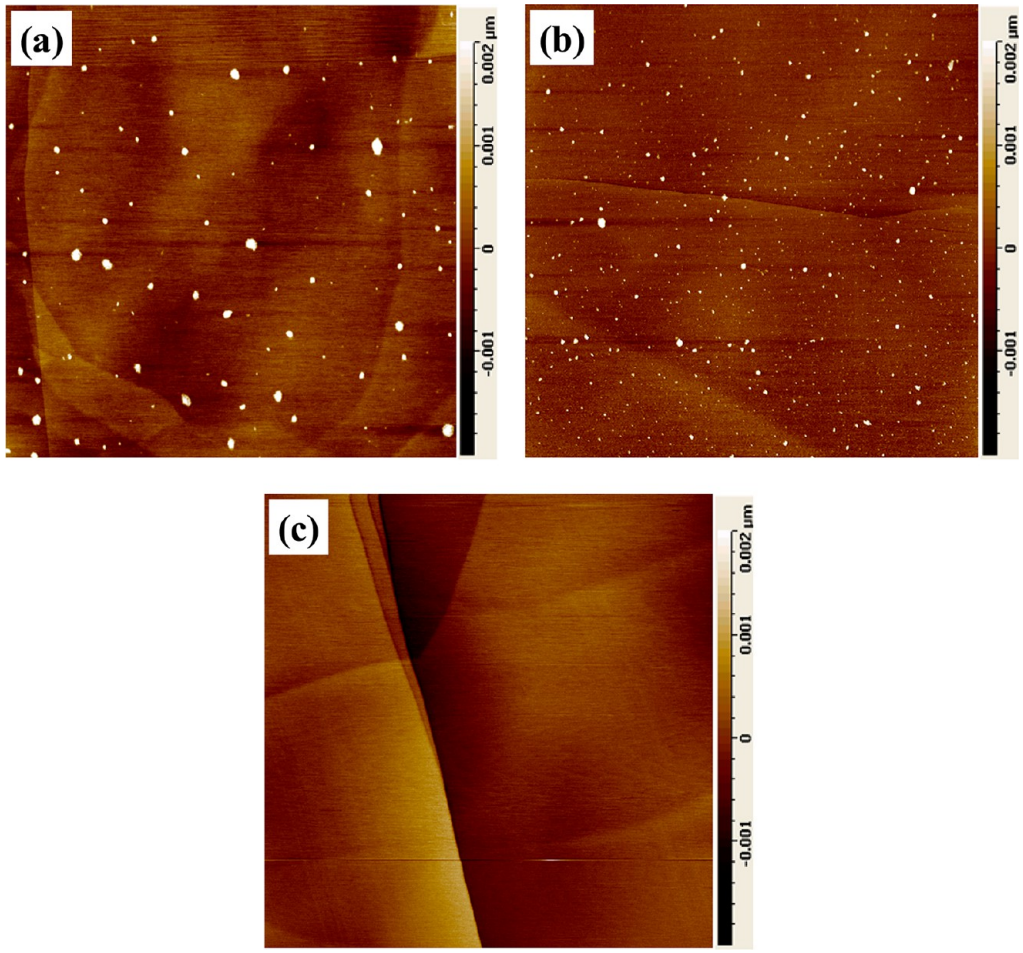

Figure 3. AFM topography images ($5 \times 5\ \mu m^2$) of surface of a HOPG substrate dipped into (a) an aged and (b) a fresh P3HT/chloroform solution and (c) a bare HOPG surface.

the surface with crystal packing in the nanowhiskers is illustrated in Figure 1d. From the amount of P3HT nanowhiskers adsorbed to the surfaces observed, it is obvious that there are attractive interactions between the substrate surface and the edge-on P3HT monolayer, and the interactions are much stronger for fluoroalkyl-functionalized surface than bared SiO_2, and much weaker for the alkyl-functionalized surface. For comparison, the same adsorption protocol was carried out using a freshly prepared P3HT chloroform solution of the same concentration. AFM revealed no P3HT adsorption on the SiO_2 and C_6H_{13} surfaces; on the C_6F_{13} surface, small P3HT aggregates of 2−4 nm thick were observed (Supporting Information). This observation is consistent with our above conclusion that the interaction between P3HT and C_6F_{13} surface is the strongest. According to the literature, the electron-withdrawing ability of surfaces decreases in order of C_6F_{13}, SiO_2, and C_6H_{13}.[15] The decreasing order of P3HT adsorption onto C_6F_{13}, SiO_2, and C_6H_{13} surfaces suggests that electron-withdrawing ability rather than surface energy[23] dominates the interactions between the surface and edge-on P3HT molecules. This finding is not in contradiction with that of ref 23. What we have demonstrated are the interactions between a surface with preformed edge-on P3HT assemblies, whereas their study involved formation of P3HT structures *in situ* on substrates by drying a P3HT solution, where surface energy of the substrate is known to be crucial to formation of ordered structure of the solutes.[26]

In addition, the absence of edge-on nanowhiskers adsorption on the alkyl-functionalized surface further confirms our previous argument that the interactions between the alkyl side chains and the alkyl surface are so weak that growth of the crystal along the side chain direction is very unfavorable, resulting in single-layer thickness in this direction.[25]

Raman spectroscopy was then employed to study the interfacial structure and interactions. Although the P3HT nanowhiskers adsorbed were of monolayer thickness, Raman signals were strong and clear. Figure 2a depicts Raman spectra of the monolayer P3HT adsorbed to different surfaces in the 600−1700 cm^{-1} region. The broad Si band at 900−1040 cm^{-1} serves as a convenient internal standard for intensity comparison between samples. The intensity of the P3HT Raman signal decreases in the order of C_6F_{13}, SiO_2, and C_6H_{13}, consistent with the amounts of P3HT adsorbed on these surfaces revealed by AFM. We focus on the highest peak located at 1440−1450 cm^{-1}, which is assigned to symmetric C═C stretching of the thiophene.[27,28] It has been reported that this band shifts to lower frequencies when the conjugation length in P3HT molecule is increased.[29] While this band emerges at 1445 cm^{-1} for a spin-coated P3HT film (Figure 2c), for nanowhiskers adsorbed, this peak is located at lower frequencies of 1440−1443 cm^{-1}, which is consistent with our previous finding that these P3HT aggregates of monolayer thickness are nanowhiskers,[25] with longer average conjugation length than P3HT in spin-coated films. However, it is intriguing

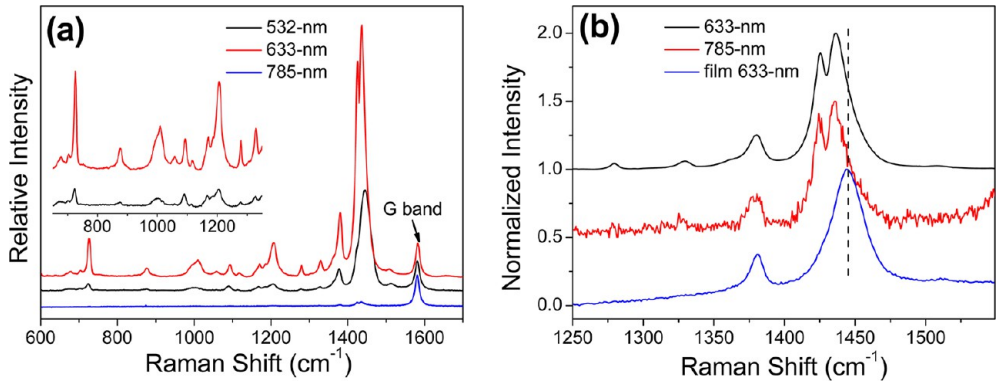

Figure 4. (a) Raman spectra obtained with 785, 633, and 532 nm excitation normalized to the G band of HOPG. (b) Spectra in the region of 1250–1550 cm^{-1} with intensities normalized for comparison; the dashed line marks the peak position of 1445 cm^{-1}.

to note that for the nanowhiskers on SiO_2 surface this peak emerges at 1440 cm^{-1}, whereas on C_6F_{13} surface it is at 1443 cm^{-1} (Figure 2). This difference cannot be due to different conjugation lengths since the nanowhiskers were formed in the same solution prior to adsorption and are expected to be of same structure. On the other hand, similar shifts in vibrational frequencies have been attributed to charge transfer.[30−33] Probably there is charge transfer between P3HT molecules and the electron-withdrawing fluoroalkyl groups on the C_6F_{13} surface, resulting in the shift of the thiophene C=C stretching peak to higher frequencies compared to that on SiO_2 surface, where such charge transfer is absent. This speculation is in line with our above conclusion that there are stronger interactions between P3HT and the C_6F_{13} surface than the SiO_2 surface.

Figure 2b shows Raman spectra for the substrates dipped into fresh P3HT solution. On the C_6F_{13} surface, much weaker P3HT peaks are observed compared to that in Figure 2a (note the relative intensity with respect to the Si peak), and on SiO_2 and C_6H_{13} surfaces P3HT is barely detected. This is again consistent with the amounts of P3HT on these surfaces observed by AFM. It is interesting that on both SiO_2 and C_6F_{13} surfaces the P3HT nanowhiskers with edge-on molecular orientation adsorbed much more than individual P3HT molecules of face-on orientation, suggesting stronger interactions of the former than the latter with the surfaces.

In photovoltaic devices, carbon materials have been widely used as electrodes, electron acceptors, and additives, the interface between which and P3HT and their interactions are crucial to device performance.[34] From perspective of structure–property relation, it is of great importance to explore the interaction in hybrids of P3HT and carbon materials. It has been reported that carbon nanotubes and reduced graphene oxide can induce P3HT crystallization, while addition of P3HT to the blends helps dispersion of carbon materials, and researchers attributed it to $\pi-\pi$ interaction at the interface.[35−37] In addition, P3HT molecules were reported to adopt face-on orientation and form "two-dimensional crystals" on the surface of highly oriented pyrolytic graphite (HOPG).[38−40] Therefore, HOPG is another surface of interest different from the functionalized SAMs. Figure 3a and 3b show AFM topography images of a HOPG substrate after being submerged into an aged and fresh P3HT chloroform solution, respectively, followed by rinsing with chloroform. A bare HOPG surface is shown in Figure 3c for comparison. P3HT aggregates of nanometer size can be identified on the HOPG surface, the morphology of which completely different from that observed on other substrates. No nanowhiskers adsorb to the surface. P3HT microcrystals with diameter of ~500 nm have been observed on single-walled carbon nanotubes (SWNTs) because of strong interactions due to charge transfer between P3HT and defects of SWNT;[41] scanning tunneling microscopy (STM) has revealed lamellae of P3HT molecules on HOPG surface with face-on orientation.[38−40] On the basis of these previous studies and the fact that edge-on nanowhiskers are absent, it may be deduced that the P3HT aggregates adsorb to HOPG surface defects with face-on orientation due to charge transfer between P3HT molecules and HOPG.

More structural information can be extracted from the Raman spectra of P3HT on HOPG surface, shown in Figure 4. They are quite different from that of P3HT on SiO_2 and C_6F_{13} surfaces and depend on excitation frequency. A close examination of the spectrum obtained with 633 nm excitation in the region of 600−1700 cm^{-1} reveals that, in addition to the G band at 1581 cm^{-1} assigned to E_{2g} vibrational mode of HOPG[42,43] and normal P3HT bands as seen in Figure 2 and Figure S2 (Supporting Information) and described previously in the literature,[28] there are several extra bands, for example 1330, 1280, 1010, 877, and 704 cm^{-1}, that have not been reported before. Normalized against the G band of HOPG at 1581 cm^{-1}, the Raman signal of P3HT is much stronger in the spectrum excited by 633 nm than 532 and 785 nm lasers, which implies that the Raman signal of P3HT on HOPG is enhanced by 633 nm excitation. Recently, researchers have revealed enhanced Raman signals for small molecules adsorbed on graphene substrate and attributed the enhancement to charge transfer between graphene and the adsorbed molecules.[44,45] On the other hand, based on the observation that carbon nanotube[35,36] and reduced graphene oxide[37] can induce P3HT crystallization, researchers have deduced that there are $\pi-\pi$ interaction and charge transfer between the two species. Therefore, it is reasonable to conclude that there are strong interactions due to charge transfer between P3HT molecule and HOPG substrate, which result in resonance enhancement of Raman signals of P3HT and consequently the appearance of some overtones and combined frequencies. In addition, in the spectrum excited at 633 nm, the C=C stretching band of P3HT shifts from 1445 cm^{-1} to lower wavenumbers and splits into a doublet at 1425 and 1436 cm^{-1}. The much greater shift of the C=C stretching band compared to that for edge-on P3HT on SAM-functionalized surfaces discussed in the previous section further supports our above conclusion of strong charge transfer interaction between face-on P3HT and

dx.doi.org/10.1021/ma302645m | Macromolecules 2013, 46, 2733−2739

HOPG surface. This kind of interaction is unlikely for edge-on P3HT molecules, and hence adsorption of the monolayer nanowhiskers is absent due to much weaker interactions between the face-on P3HT monolayer adsorbed on the HOPG surface and the alkyl side chains on the flat facets of the nanowhiskers. Along this line of argument, it is also reasonable to argue that the white dots on HOPG are face-on P3HT crystallites. A split in the C=C stretching band is also clearly seen in the spectrum excited by 785 nm similar to that by 633 nm excitation, indicating that the appearance of an additional component here is not due to resonance enhancement, but can be attributed to two kinds of P3HT molecules on the HOPG substrate: the face-on P3HT monolayer ("two-dimensional crystals"[38]) detected by STM (Figure S3) that is not seen by AFM and the nanometer size aggregates.

■ CONCLUSION

In this work, using P3HT nanowhiskers of monolayer thickness grown in solution as a probe, we are able to directly explore the interfacial interactions between P3HT and dielectric surfaces by studying the adsorption of the preformed P3HT monolayer to the substrates by AFM and Raman. We found that the interaction between P3HT molecules in edge-on orientation with substrate surface is dominated by the electron-withdrawing ability of the surface functional groups. In particular, surface with fluorocarbon functionalities favors adsorption of edge-on P3HT molecules, possibly via some extent of charge transfer. On the HOPG surface, on the other hand, strong charge transfer interaction between the surface and the thiophene rings is present, as evidenced by the resonance enhancement of Raman signals and shift of the thiophene ring vibration peak, which favors face-on adsorption of P3HT molecules and excludes edge-on adsorption of P3HT. These findings can help guide the interface engineering in polythiophene-based optoelectronic devices for improved performance.

■ ASSOCIATED CONTENT

Supporting Information

AFM topography images of P3HT adsorption on C_6F_{13} from fresh P3HT/chloroform solution and Raman spectrum of spin-coated P3HT film excited by 633 nm laser; STM image of "2D P3HT crystals" formed on HOPG. This material is available free of charge via the Internet at http://pubs.acs.org.

■ AUTHOR INFORMATION

Corresponding Author

*Ph +86-431-85262854; Fax +86-431-85262126; e-mail zhsu@ciac.jl.cn.

Notes

The authors declare no competing financial interest.

■ ACKNOWLEDGMENTS

The financial support from the National Natural Science Foundation of China (20990233) is acknowledged. Z.S. thanks the NSFC Fund for Creative Research Groups (50921062) for support.

■ REFERENCES

(1) Facchetti, A. *Chem. Mater.* **2011**, *23*, 733.
(2) Beaujuge, P. M.; Frechet, J. M. J. *J. Am. Chem. Soc.* **2011**, *133*, 20009.
(3) Park, Y. D.; Lim, J. A.; Lee, H. S.; Cho, K. *Mater. Today* **2007**, *10*, 46.
(4) Klauk, H. *Chem. Soc. Rev.* **2010**, *39*, 2643.
(5) Brady, M. A.; Su, G. M.; Chabinyc, M. L. *Soft Matter* **2011**, *7*, 11065.
(6) Kline, R. J.; McGehee, M. D. *Polym. Rev.* **2006**, *46*, 27.
(7) Campoy-Quiles, M.; Ferenczi, T.; Agostinelli, T.; Etchegoin, P. G.; Kim, Y.; Anthopoulos, T. D.; Stavrinou, P. N.; Bradley, D. D. C.; Nelson, J. *Nat. Mater.* **2008**, *7*, 158.
(8) Sun, Y.; Liu, J. G.; Geng, Y. H.; Han, Y. C. *Chin. J. Appl. Chem.* **2012**, *29*, 1399.
(9) Sun, X. N.; Di, C. A.; Liu, Y. Q. *J. Mater. Chem.* **2010**, *20*, 2599.
(10) Kim, F. S.; Ren, G.; Jenekhe, S. A. *Chem. Mater.* **2011**, *23*, 682.
(11) Lunt, R. R.; Osedach, T. P.; Brown, P. R.; Rowehl, J. A.; Bulovic, V. *Adv. Mater.* **2011**, *23*, 5712.
(12) Wang, S. H.; Kiersnowski, A.; Pisula, W.; Mullen, K. *J. Am. Chem. Soc.* **2012**, *134*, 4015.
(13) Kline, R. J.; Mcgehee, M. D.; Toney, M. F. *Nat. Mater.* **2006**, *5*, 222.
(14) Halik, M.; Hirsch, A. *Adv. Mater.* **2011**, *23*, 2689.
(15) Kobayashi, S.; Nishikawa, T.; Takenobu, T.; Mori, S.; Shimoda, T.; Mitani, T.; Shimotani, H.; Yoshimoto, N.; Ogawa, S.; Iwasa, Y. *Nat. Mater.* **2004**, *3*, 317.
(16) Jang, Y.; Cho, J. H.; Kim, D. H.; Park, Y. D.; Hwang, M.; Cho, K. *Appl. Phys. Lett.* **2007**, *90*, 132104.
(17) Pernstich, K. P.; Haas, S.; Oberhoff, D.; Goldmann, C.; Gundlach, D. J.; Batlogg, B.; Rashid, A. N.; Schitter, G. *J. Appl. Phys.* **2004**, *96*, 6431.
(18) Calhoun, M. F.; Sanchez, J.; Olaya, D.; Gershenson, M. E.; Podzorov, V. *Nat. Mater.* **2008**, *7*, 84.
(19) Sirringhaus, H.; Brown, P. J.; Friend, R. H.; Nielsen, M. M.; Bechgaard, K.; Langeveld-Voss, B. M. W.; Spiering, A. J. H.; Janssen, R. A. J.; Meijer, E. W.; Herwig, P.; de Leeuw, D. M. *Nature* **1999**, *401*, 685.
(20) Kim, D. H.; Park, Y. D.; Jang, Y. S.; Yang, H. C.; Kim, Y. H.; Han, J. I.; Moon, D. G.; Park, S. J.; Chang, T. Y.; Chang, C. W.; Joo, M. K.; Ryu, C. Y.; Cho, K. W. *Adv. Funct. Mater.* **2005**, *15*, 77.
(21) Kim, D. H.; Jang, Y.; Park, Y. D.; Cho, K. *Langmuir* **2005**, *21*, 3203.
(22) Kim, D. H.; Jang, Y.; Park, Y. D.; Cho, K. *Macromolecules* **2006**, *39*, 5843.
(23) Anglin, T. C.; Speros, J. C.; Massari, A. M. *J. Phys. Chem. C* **2011**, *115*, 16027.
(24) Malliaras, G. G.; Lyashenko, D. A.; Zakhidov, A. A.; Pozdin, V. A. *Org. Electron.* **2010**, *11*, 1507.
(25) Guo, Y.; Jiang, L.; Ma, X. J.; Hu, W. P.; Su, Z. H., submitted for publication.
(26) Han, W.; Lin, Z. Q. *Angew. Chem., Int. Ed.* **2012**, *51*, 1534.
(27) Louarn, G.; Trznadel, M.; Buisson, J. P.; Laska, J.; Pron, A.; Lapkowski, M.; Lefrant, S. *J. Phys. Chem.* **1996**, *100*, 12532.
(28) Baibarac, M.; Lapkowski, M.; Pron, A.; Lefrant, S.; Baltog, I. *J. Raman Spectrosc.* **1998**, *29*, 825.
(29) Tsoi, W. C.; James, D. T.; Kim, J. S.; Nicholson, P. G.; Murphy, C. E.; Bradley, D. D. C.; Nelson, J.; Kim, J. *J. Am. Chem. Soc.* **2011**, *133*, 9834.
(30) Matsuzaki, S.; Kuwata, R.; Toyoda, K. *Solid State Commun.* **1980**, *33*, 403.
(31) Rao, A. M.; Eklund, P. C.; Bandow, S.; Thess, A.; Smalley, R. E. *Nature* **1997**, *388*, 257.
(32) Thompson, W. H.; Hynes, J. T. *J. Am. Chem. Soc.* **2000**, *122*, 6278.
(33) Smothers, W. K.; Wrighton, M. S. *J. Am. Chem. Soc.* **1983**, *105*, 1067.
(34) Dai, L. M.; Chang, D. W.; Baek, J. B.; Lu, W. *Small* **2012**, *8*, 1130.
(35) Liu, J. H.; Zou, J. H.; Zhai, L. *Macromol. Rapid Commun.* **2009**, *30*, 1387.
(36) Geng, J. X.; Kong, B. S.; Yang, S. B.; Youn, S. C.; Park, S.; Joo, T.; Jung, H. T. *Adv. Funct. Mater.* **2008**, *18*, 2659.

(37) Chunder, A.; Liu, J.; Zhai, L. *Macromol. Rapid Commun.* **2010**, *31*, 380.
(38) Mena-Osteritz, E.; Meyer, A.; Langeveld-Voss, B. M. W.; Janssen, R. A. J.; Meijer, E. W.; Bauerle, P. *Angew. Chem., Int. Ed.* **2000**, *39*, 2680.
(39) Grevin, B.; Rannou, P.; Payerne, R.; Pron, A.; Travers, J. P. *Adv. Mater.* **2003**, *15*, 881.
(40) Grevin, B.; Rannou, P.; Payerne, R.; Pron, A.; Travers, J. P. *J. Chem. Phys.* **2003**, *118*, 7097.
(41) Geng, J. X.; Zeng, T. Y. *J. Am. Chem. Soc.* **2006**, *128*, 16827.
(42) Allen, M. J.; Tung, V. C.; Kaner, R. B. *Chem. Rev.* **2010**, *110*, 132.
(43) Wang, Y.; Alsmeyer, D. C.; Mccreery, R. L. *Chem. Mater.* **1990**, *2*, 557.
(44) Ling, X.; Xie, L. M.; Fang, Y.; Xu, H.; Zhang, H. L.; Kong, J.; Dresselhaus, M. S.; Zhang, J.; Liu, Z. F. *Nano Lett.* **2010**, *10*, 553.
(45) Ling, X.; Zhang, J. *Small* **2010**, *6*, 2020.